Arch. Metall. Mater. **69** (2024), 2, 395-400

DOI: https://doi.org/10.24425/amm.2024.149753

YEO-UL SONG[1*], BYEONG UK SONG[2], JOON PHIL CHOI[3], MIN-KYO JUNG[3], TAEHO HA[3], PIL-HO LEE[3]

OPTIMIZING TIME-CONSTRAINED MULTI-OBJECTIVE PROCESS PARAMETERS FOR THIN-WALLED MARAGING STEELS MANUFACTURED BY LASER POWDER BED FUSION (LPBF)

Additive manufacturing is an innovative manufacturing process that enables complex topological structures and low-volume, high-variety production. One of the major adaptations of this method is in the tire industry. Thin-walled sipes slit the tires to improve drainage and traction. The material properties of thin-walled structures manufactured by additive manufacturing are different and more sensitive than those of conventional cube-shaped specimens. Thin-walled maraging steel specimens are considered to be able to model the relationship between the process parameters and the properties of the sipes adequately. Tire sipes are made of maraging steel. Maraging steels are a class of low-carbon high-alloy martensitic steel generally providing high strength, ductility, and good fracture toughness. In particular, these alloys exhibit a good combination of strength and toughness at elevated temperatures, which has been desirable for applications in aerospace and tooling. In order to consider productivity, multi-objective process parameter optimization with a build-time-constrained model is proposed.

Keywords: Additive manufacturing; Machine learning; Multi-objective optimization; LPBF (Laser Powder Bed Fusion)

1. Introduction

Additive manufacturing creates new trends in the manufacturing industry and enables the realization of items not possible to create with traditional methods. Many companies in various fields, including the aerospace, automotive, and medical industries, are starting to adopt additive manufacturing to increase their productivity [1]. Each product requires its own process window for the new additive manufacturing system prior to actual mass production. In additive manufacturing, dozens of input process parameters affect the resulting material properties [2]. However, the relationship between the input parameters and the output material properties cannot be explicitly expressed. Many studies have proposed data-driven models to find optimal process parameters for their target material properties [3-5]. The relative density value is the most important factor, as it indicates whether the product will be formed well. Existing studies have considered cube-shaped coupons for creating test additive manufacturing samples [6-8]. This study focuses on tire sipes, and because tire sipes are considered as final products, thin-walled specimens are adopted in this study. There are several ways to obtain the density value, but the Archimedes method is the most popular due to its simplicity. However, the Archimedes approach is sensitive to environmental factors, such as the types and temperatures of any liquids involved, and the shape of the coupon [9]. For additively manufactured samples, the Archimedes density values for thin-walled specimens and cubes are different. Therefore, thin-walled specimens require a new process map [10].

The role of the sipe is to make a thin slit in the rubber tire to improve drainage and increase tire traction. Maraging steel (MS1) with excellent strength and toughness is used for tire sipes. Because the sipe must withstand high pressure during the pressing process, it must have high density and good strength. In order to maximize durability and productivity, the density and strength are set as objective functions and the build time is set as a constraint. The present work is dedicated to the construction of a time-constrained multi-objective optimization model for LPBF process parameters.

2. Experimental

Tire sipes are made of maraging steel (MS1) due to their high strength requirements [11]. The specimens in the present

[1] KOREA INSTITUTE OF MACHINERY & MATERIALS, DEPARTMENT OF INDUSTRIAL MACHINERY DX, 156 GAJEONGBUK-RO, YUSEONG-GU, DAEJEON 34103, REPUBLIC OF KOREA
[2] KAIST, REPUBLIC OF KOREA
[3] KOREA INSTITUTE OF MACHINERY & MATERIALS, DEPARTMENT OF 3D PRINTING, 156 GAJEONGBUK-RO, YUSEONG-GU, DAEJEON 34103, REPUBLIC OF KOREA

* Corresponding author: yeoulsong@kimm.re.kr

work were built using an EOS290 device with maraging steel (MS1) powder. TABLE 1 shows the chemical composition of the MS1 powder. The powder particle size distribution is 18 μm, 35 μm, and 54 μm for D10, D50, and D90, respectively [12,13]. Fig. 1(a) shows a specimen printed with dimensions of 50 mm × 1 mm × 20 mm. Using this coupon, dog-bone-shaped tensile specimens for a strength test were fabricated, as shown in Fig. 1(b). The Archimedes method is used for the density data and a 25 kN universal testing machine is used for the strength data. Tensile stress-strain curves are obtained at room temperature and a displacement rate of 1mm/min. Using the functions provided by EOS290, the time required to build a 100 mm × 100 mm × 100 mm cube was used as the build-time data input parameter.

TABLE 1

Chemical Composition of the MS1 Powder

Element	Ni	Co	Mo	Ti	Al	Si	C	Fe
Percent	18.15	9.04	4.81	0.67	0.10	0.011	0.0076	Balance

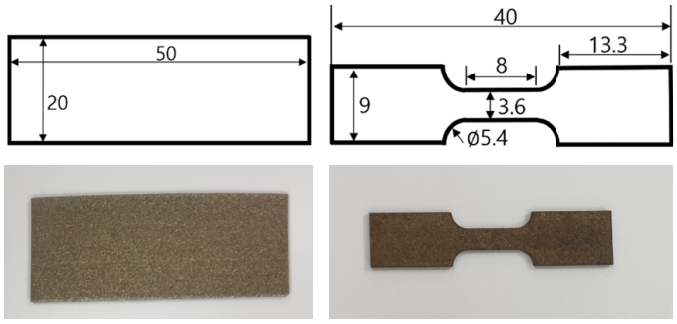

(a) Printed specimen shape (b) Dog-bone-shaped tensile specimen

Fig. 1. Specimen shape for (a) relative density and (b) tensile strength

Three process parameters are considered: the laser power, laser scanning speed, and hatch distance. The laser power range is 190 W to 370 W, the laser scanning speed range is 700 to 1600 mm/s, and the hatch distance and is 0.09 mm to 0.13 mm.

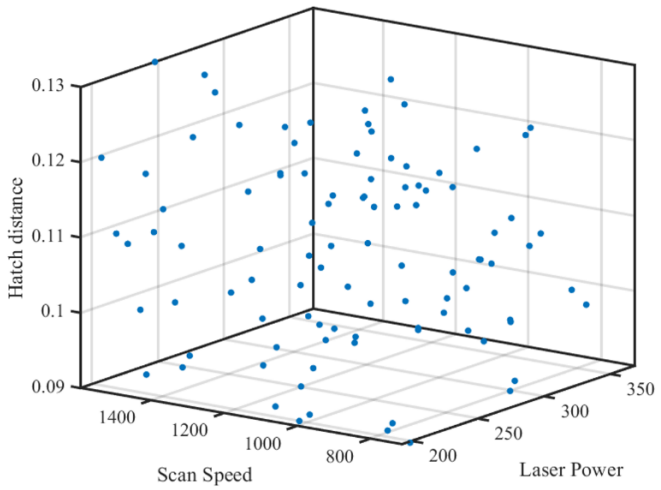

Fig. 2. Design of experiments (DoE) using LHS for collection of training data

A stripe scan pattern with 67° rotation from layer to layer is used to reduce sample anisotropy. Using Latin hypercube sampling (LHS), 100 uniformly distributed sample points were extracted, as shown in Fig. 2.

3. Results and discussion

In order to construct the surrogate model for the relationship between the input process parameters and the output material properties, Gaussian process regression (GPR) is utilized. GPR is a probabilistic and non-parametric regression model. The input x and output y are expressed as shown below, and ε is the noise, which takes the form of a Gaussian distribution.

$$y = f(x) + \varepsilon$$

GPR considers correlations in the training data to represent reasonable predictions for new input. In order to predict y^* and at a new point x^*, the Gaussian process of training data y is needed because y^* follows a multi-variate Gaussian distribution, as follows:

$$\begin{bmatrix} y \\ y^* \end{bmatrix} \sim N\left(\mu, \sigma^2\right)$$

where

$$\mu = 0,\ \sigma^2 = \begin{bmatrix} k(x,x) & k(x,x') \\ k(x',x) & k(x',x') \end{bmatrix}$$

Here, k is a kernel function that represents the covariance between the input x values.

In this study, 100 training samples were utilized, as shown in Fig. 2. The training data values of the density and tensile strength are expressed as plots, and the predicted data-driven model is expressed as a mesh. Fig. 3 shows the GPR models constructed using build-time data provided by EOS290 when entering the training data process parameters. GPR models are constructed for the relative density, tensile strength, and build-time training data, respectively.

To optimize these outputs such as relative density and tensile strength while considering building time, the multi-objective optimization problem is used. The standard multi-objective optimization problem is defined as [14]:

$$\text{To minimize } \boldsymbol{c}(\boldsymbol{x}) = \left[c_1(\boldsymbol{x}), c_2(\boldsymbol{x}), \ldots, c_i(\boldsymbol{x}), \ldots, c_p(\boldsymbol{x})\right]^T$$

$$\text{Subject to } h_m(\boldsymbol{x}) = 0, \quad m = 1,2,\ldots,q$$

$$g_n(\boldsymbol{x}) \le 0,\ n = 1,2,\ldots,r$$

$$\boldsymbol{x}^{LB} \le \boldsymbol{x} \le \boldsymbol{x}^{UB}$$

where $c_i(\boldsymbol{x})$ is the i^{th} objective function and p, q, r is the number of objective functions, equality constraints, and inequality constraints, respectively. In this research, two objective functions, such as relative density and tensile strength, and one inequality constraint, such as building time, are used. And weighted sum,

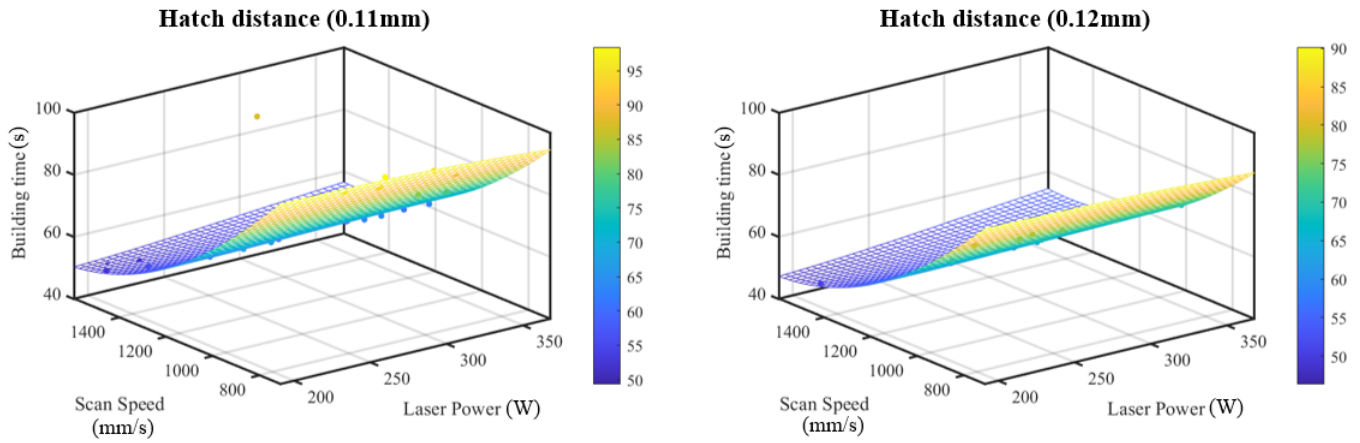

Fig. 3. GPR model predictions between the input process parameters and build-time at hatch distances of (a) 0.11 mm and (b) 0.12 mm

one of the methods to define the multi-objective optimization problem, is applied to the objective function. Then, the optimization formulation in this research using GPR surrogate model can be shown as follows:

$$\text{To minimize } w_1\tilde{c}_1(\boldsymbol{x}) + w_2\tilde{c}_2(\boldsymbol{x})$$

$$\text{Subject to } \tilde{g}(\boldsymbol{x}) \le 0$$

$$\boldsymbol{x}^{LB} \le \boldsymbol{x} \le \boldsymbol{x}^{UB}$$

where $w_1 + w_2 = 1$, $\tilde{c}_1(\boldsymbol{x})$, $\tilde{c}_2(\boldsymbol{x})$, and $\tilde{g}(\boldsymbol{x})$ are GPR surrogate models with relative density, tensile strength, and building time, respectively. $\boldsymbol{x}^{LB}$ and $\boldsymbol{x}^{UB}$ are the lower and upper bounds of input parameters, respectively. As the weight changes, several optimal points may exist. To find these optimal points, the Pareto optimal set can be used. The Pareto optimal set finds the set of the optimal points, changing the weights. Then, we can determine the optimal point among these optimal sets [15].

A genetic algorithm (GA) is used to find the optimal input process parameters and is based on the natural selection process. Fig. 4 shows the proposed data-driven machine learning models for the process parameters and the relative density and yield stress properties. The proposed models are shown in Fig. 4. The proposed surrogate models are shown in Fig. 4 at hatch distances of 0.1, 0.11 and 0.12 that takes into account the three variables of the laser power, laser scan speed, and hatch distance. In general, the lower the speed and hatch distance values are, the higher the density and tensile strength levels become, as shown in Fig. 4. In Fig. 4, the red points represent several optimized points at approximately the lowest laser scan speed, as mentioned above. The optimal process parameters are the power of 274 W, a laser scan speed of 813 mm/s, a hatch distance of 0.1 mm, and a corresponding predicted relative density of 97.6% and yield strength of 934 N/mm^2. At these optimal values in Fig. 4, the energy density values are around 81~74 J/mm^3, and these results are convincing when compared to other MS1 additive printing studies [6]. However, productivity, which is directly related to income, is also a major consideration in actual industries. Fig. 5 shows the optimal process points with build-time constraints at the level of about 70% of the maximum build time. Optimal process parameters are shifted into the interior design area, where the laser scan speed and hatch distance are greater compared to those in the unconstrained optimization results, as shown in Fig. 5. The optimal process parameters for the time-constrained model are the power of 256 W, a laser scan speed of 1136 mm/s, a hatch distance of 0.1mm and a corresponding predicted relative density level of 96.9% and yield strength of 915 N/mm^2. Compared to the unconstrained optimization result, the constrained result shows a higher laser scan speed but lower density and strength values. Given the time constraints, it is necessary to ensure that the optimized parameters satisfy the target properties of the material.

Based on this proposed time-constrained multi-objective surrogate model, users can find their own process parameters taking into account the target material properties and economic margin.

4. Conclusions

Additive manufacturing is changing the face of the manufacturing industry at present because it is advantageous for shape representation and enables high-variety low-volume production. However, the primary considerations of industry are meeting material specifications and high productivity. The proposed method presents a surrogate model for obtaining optimal process parameters that satisfy material property requirements and build-time constraints.

Acknowledgments

This research was supported by a grant of the Basic Research Program funded by the Korea Institute of Machinery and Materials (grant No. NK248I) and the framework of international cooperation program managed by the National Research Foundation of Korea (NRF-2022K1A3A1A61015007).

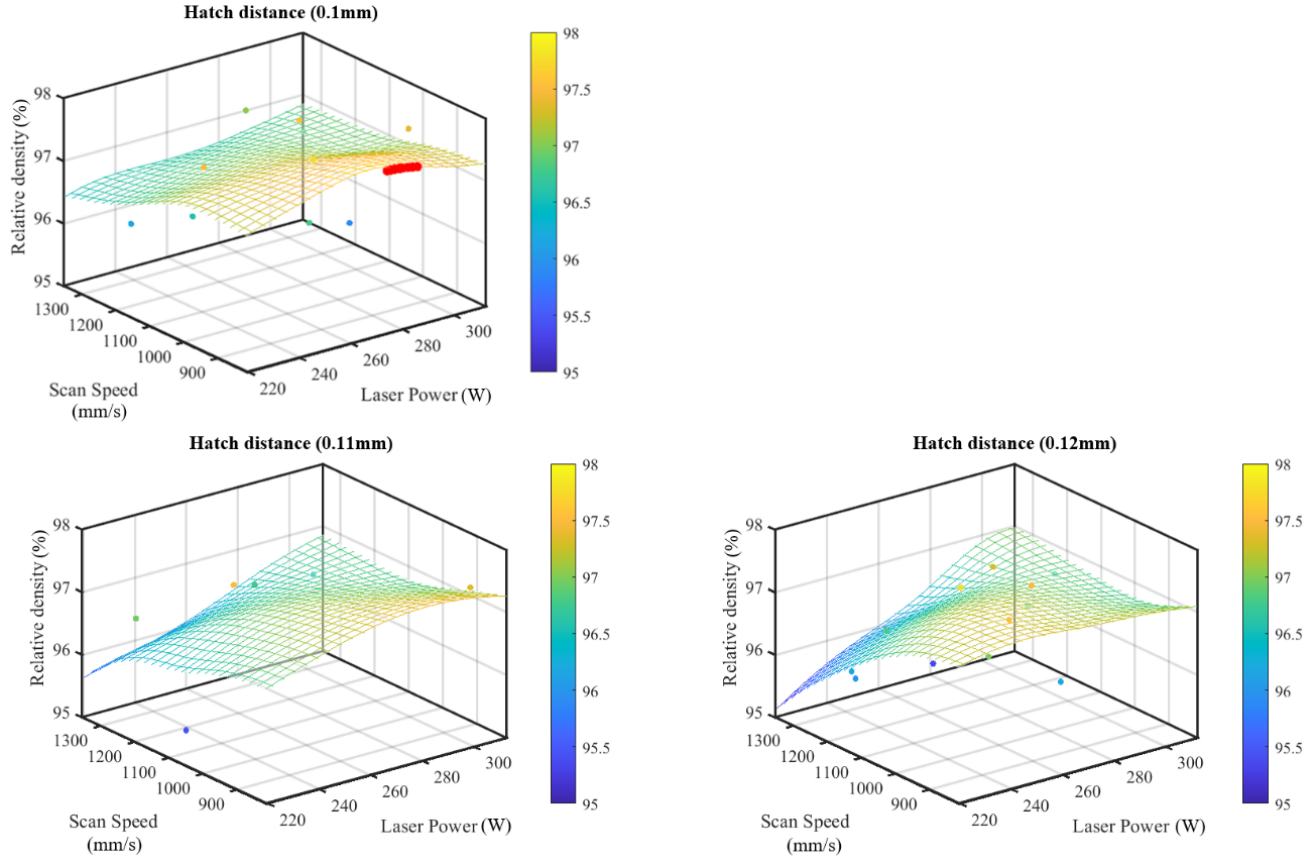

(a) GPR model predictions of relative density

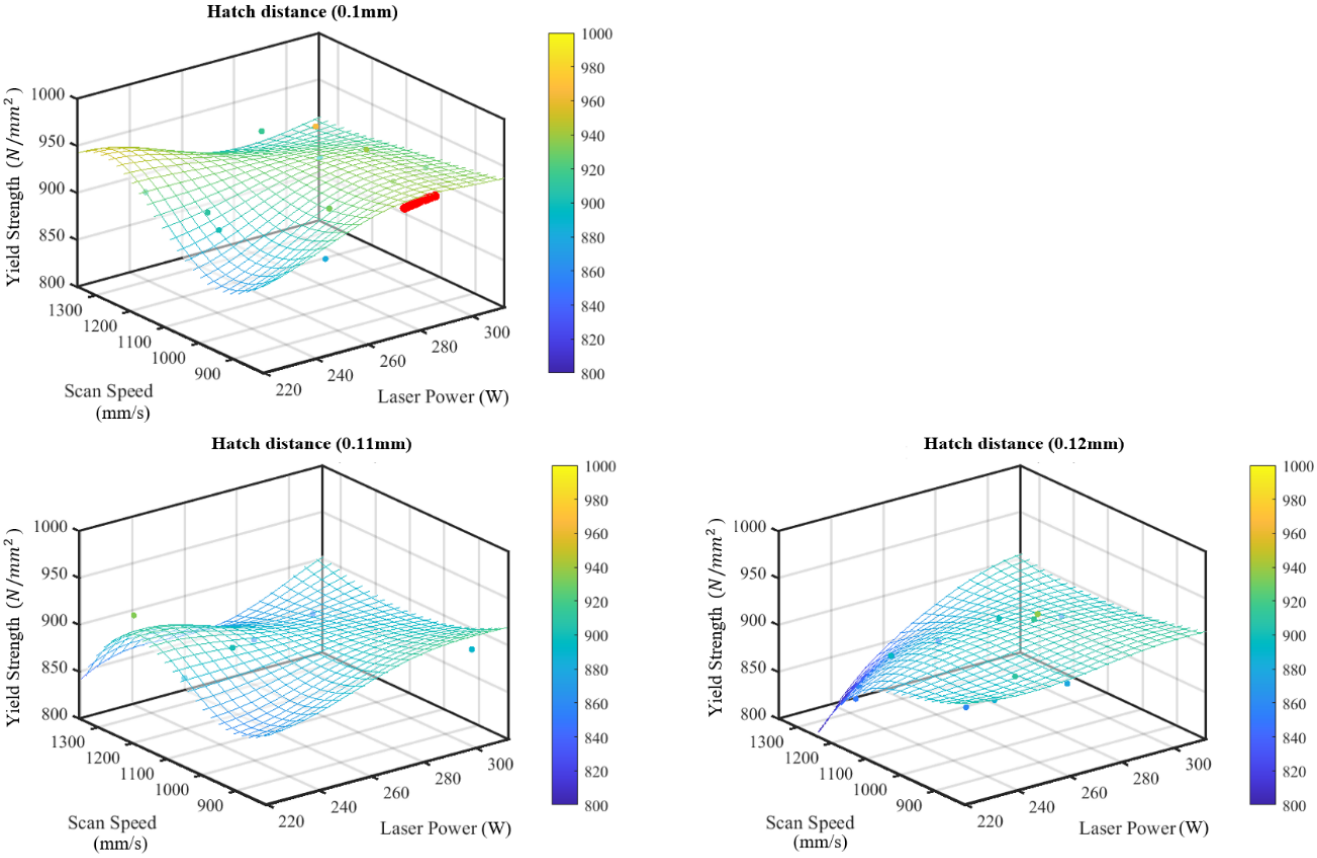

(b) GPR model predictions of Yield strength

Fig. 4. Results of multi-objective optimization using GA without time constraint and optimal locations of the process parameters, red dot means Pareto optimal points: (a) relative density and (b) Yield strength

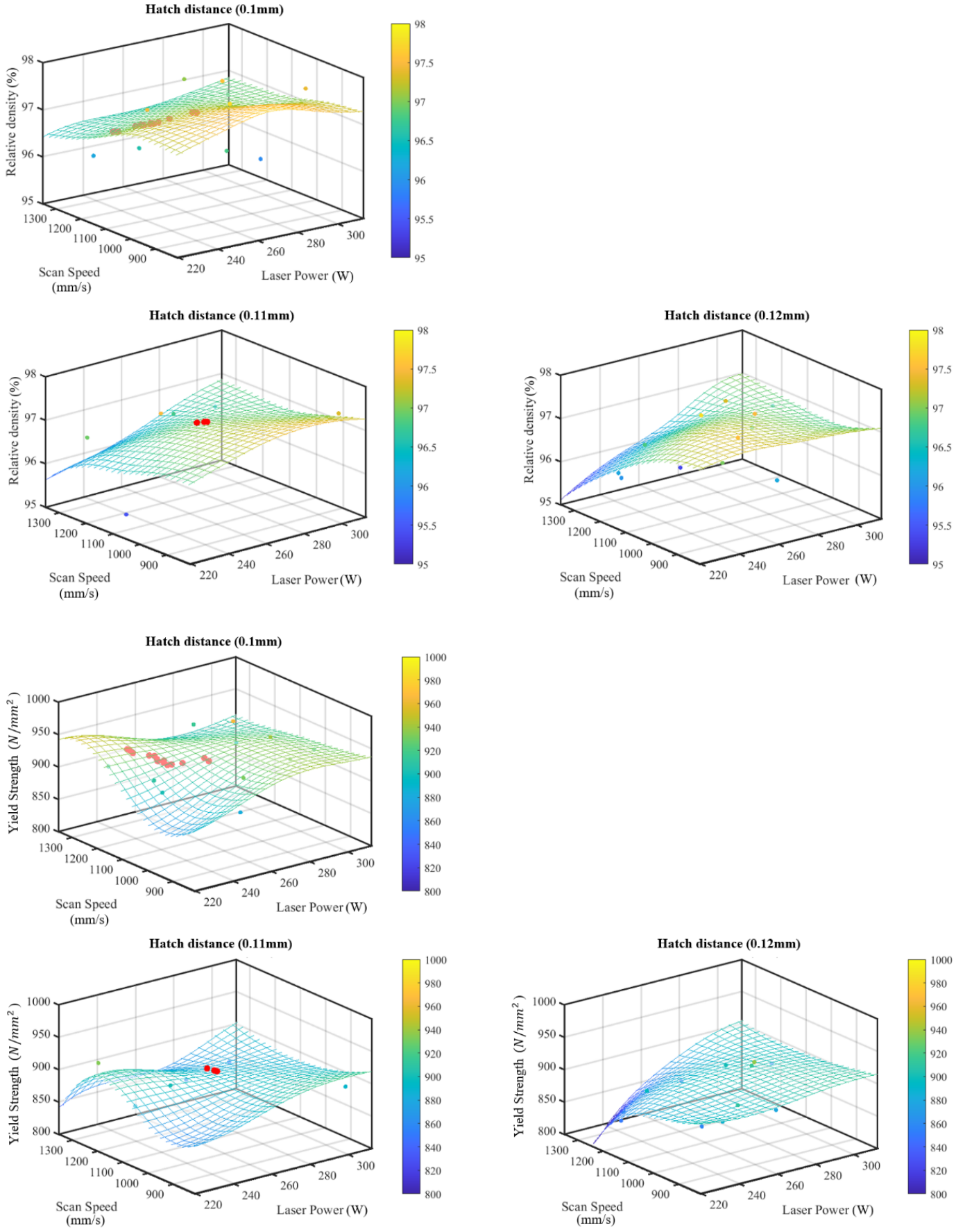

Fig. 5. Results of time-constrained multi-objective optimization using GA and optimal locations of the process parameters, red dot means the Pareto optimal points

REFERENCES

[1] https://www.michelin.com/en/activities/high-tech-materials/3d-printing/

[2] B.S. Rao, T.B. Rao, Effect of Process Parameters on Powder Bed Fusion Maraging Steel 300: A Review. Lasers in Manufacturing and Materials Processing **9** (3), 338-375 (2022).

[3] J. Li, J. Hu, L. Cao, S. Wang, H. Liu, Q. Zhou, Multi-objective process parameters optimization of SLM using the ensemble of metamodels. J. Manuf. Processes **68** (2021).

[4] H. Zhang, J.P. Choi, S.K. Moon, T.H. Ngo, A multi-objective optimization framework for aerosol jet customized line width printing via small data set and prediction uncertainty. J. Mater. Process. Technol. **116779** (2020).

[5] P. Kundo, K. Youngsoo, K. Minki, S. Chihyeon, P. Jinkyoo, R. Seunghwa, Designing staggered platelet composite structure with Gaussian process regression based Bayesian optimization. Composites Science and Technology **220** (2022).

[6] Y. Deng, Z. Mao, N. Yang, X. Niu, X. Lu, Collaborative optimization of density and surface roughness of 316L stainless steel in selective laser melting. Materials **13** (7), 1601 (2020).

[7] A. Suzuki, R. Nishida, N. Takata, M. Kobashi, M. Kato, Design of laser parameters for selectively laser melted maraging steel based on deposited energy density, Additive Manufacturing **28**, 160-168 (2019).

[8] M. Yonehara, T.T. Ikeshoji, T. Nagahama, T. Mizoguchi, M. Tano, T. Yoshimi, H. Kyogoku, Parameter optimization of the high-power laser powder bed fusion process for H13 tool steel. The International Journal of Advanced Manufacturing Technology **110**, 427-437 (2020).

[9] T. de Terris, O. Andreau, P. Peyre, F. Adamski, I. Koutiri, C. Gorny, C. Dupuy, Optimization and comparison of porosity rate measurement methods of Selective Laser Melted metallic parts. Additive Manufacturing **28**, 802-813 (2019).

[10] C. Chen, Z. Xiao, H. Zhu, Deformation and control method of thin-walled part during laser powder bed fusion of Ti–6Al–4V alloy. Int. J. Adv. Manuf. Technol. **110** (2020).

[11] H. Weidong, Z. Weijie, C. Xiayu, Effect of SLM Process Parameters on Relative Density of Maraging Steel (18Ni-300) Formed Parts, **774**, 2020 IOP Conf. Ser.: Mater. Sci. Eng. (2020)

[12] EOS, Material data sheet EOS MaragingSteel MS1.

[13] H. Azizi, R. Ghiaasiaan, R. Prager, M.H. Ghoncheh, Khaled Abu Samk, Ante Lausic, Wes Byleveld, A.B. Phillion, Metallurgical and mechanical assessment of hybrid additively-manufactured maraging tool steels via selective laser melting. Additive Manufacturing **27** (2019).

[14] C.A.C. Coello, G.B. Lamont, D.A. Van Veldhuizen, Evolutionary algorithms for solving multi-objective problems. New York: Springer **5**, 79-104 (2007).

[15] K. Deb, Multi-objective optimisation using evolutionary algorithms: an introduction, Multi-objective evolutionary optimisation for product design and manufacturing. Springer **3-34**, London (2011).